GQuEST Control System Resolution

David Nguyen[1,2] and Chris Stoughton[3]
[1)] *Physics Department, Colorado School of Mines*
[2)] *Scientific Undergraduate Laboratory Intern, Fermilab 2024*
[3)] *Fermilab Scientist*

(Dated: July 26, 2024)

GQuEST (Gravity from Quantum Entanglement of Space-Time), is a collaboration verifying a quantum gravity model by measuring holographic effects on a microscopic scale. Its interferometer apparatus filters excessive optical noise and requires a control system that can adjust the filtration to accommodate for frequency changes in the output light. We stress-test this control system by simulating filter behaviors with parameters in their outermost regimes, and we have determined a threshold that maintains precision while minimizing resource usage. These results are important for the successful operation of GQuEST's interferometer, enabling more accurate tests of quantum gravity models and thereby advancing our understanding of gravity at the quantum mechanical level.

I. THEORETICAL BACKGROUND

Within the last century, one of the most prevailing challenges in theoretical physics has been developing a quantum description of gravity. On one hand, physicists have come to understand gravity as curvature of the spacetime background due to the presence of energy and momentum. On the other, quantum mechanics has supplied a framework regarding the behavior of particles on a fundamental level. Though both are powerful formalisms in their own right, together, they have proven to be structurally incompatible with one another. From gravity's non-linearity to its background independence, numerous barriers have shown to be conflicting with attempts to formulate it within a quantum mechanical framework. Another issue associated with understanding quantum gravity is its detectability. As gravity is measurable within an energy and length scale drastically larger than that of quantum mechanics, observing gravity's local behavior has proven to be another conundrum in modeling.

In more recent years, one established development in this field of theoretical physics is holography, which delineates a discrepancy in the degrees of freedom describing gravitational models and quantum mechanical models. A result of String Theory, the holographic principle has become renowned for its appealing mathematical simplification and applications in condensed matter physics. Building on its insights, Verlinde and Zurek posit that by applying this concept locally, there are hypothetically discoverable fluctuations in longitudinal distances. These fluctuations are due to variations in the vacuum energy which arise from holographic degrees of freedom. GQuEST (Gravity from Quantum Entanglement of Space-Time) is a collaboration that seeks to verify this holographic conjecture and address the challenge of detecting quantum gravity.[1,2]

II. EXPERIMENTAL BACKGROUND

To confront these challenges, GQuEST is constructing a sophisticated setup design to probe and measure these fluctuations. The apparatus consists of two co-located highly sensitive Michelson-Morley interferometers. Interferometers have been chosen as the primary measuring tool, because the predicted metric fluctuations are expected to induce changes in distances, resulting in noticeable optical interferences. The two interferometers are used to distinguish signals correlated with the metric fluctuation and uncorrelated noise. Additionally, the setup includes both homodyne readout and superconducting nanowire single-photon detection, with the latter intended to mitigate the quantum shot-noise that limits the effectiveness of the former. Details shown in figures 1 and 2.[3]

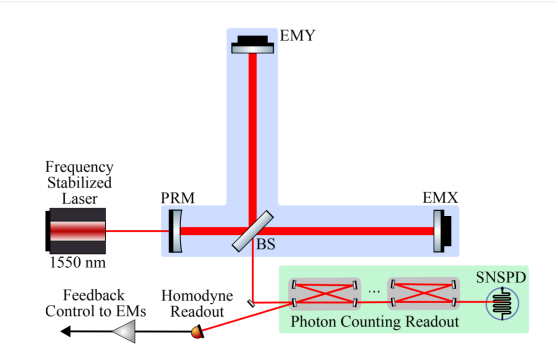

FIG. 1. Simplified experimental design of single interferometer (IFO). A 1550 nm laser inputs light into the power-recycling cavity comprised of the power-recycling mirror (PRM), the incidental beamsplitter (BS), and end mirrors (EMX, EMY). The output light is sifted through narrow-band filter-cavities. The superconducting nanowire single-photon detector (SNSPD) detects the filtered photons. The homodyne readout scheme uses the light from the first filter cavity for feedback control of the IFO.[3]

Moreover, also included in the apparatus are multiple narrowband filter cavities. These are meant to block carrier light to allow for sensitive detection of light modulated by the Verlinde and Zurek effect. These cavities will be adjusted in length based on the frequency of the output light in order ensure the most optimal filtering.

III. RESEARCH OBJECTIVES

The filter cavities will be adjusted in length using a digital control system comprised of field programmable gate arrays

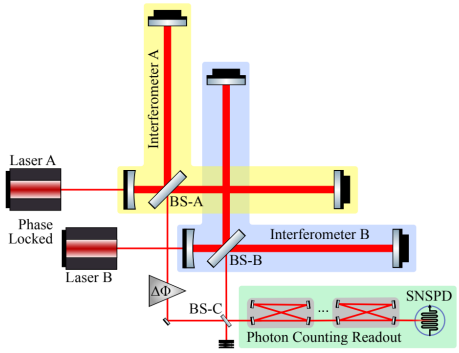

FIG. 2. Simplified experimental design of twin interferometer. The setup involves interfering light from the two interferometers, where the difference between coherent and incoherent signals provides an estimate of the geontropic signal. The system's detection efficiency improved by combining outputs from both interferometers, where $\Delta\Phi$ is a adjustable phase ensuring appropriate interference.[3]

(FPGA). It is crucial for these FPGAs to have sufficient bit resolution to maintain measurement precision from the interferometers while minimizing the usage of resources. My goal is to determine the optimal bit resolution that strikes a balance between precision and resource efficiency, ensuring accurate measurements without overburdening the system.

IV. DIGITAL SIGNAL PROCESSING

To ensure the proper functionality of the FPGAs, we stress-test the behavior of the control system through simulations of digital filtering processes, specifically focusing on a biquadratic filter. This 2^{nd} order iterative filter is characterized by five coefficients: a_1, a_2, b_0, b_1, and b_2. The particular values assigned to these coefficients can produce various filters including (but not limited to) low-pass, high-pass, and band-stop filters. The coefficients are applied into the following difference equations alongside the input signal, and the output signal is then attained by iterating over the n values.

$$y_n = b_0 w_n + b_1 w_{n-1} + b_2 w_{n-2} \tag{1}$$

$$w_n = x_n + a_1 w_{n-1} + a_2 w_{n-2} \tag{2}$$

For our tests, we specifically stress-test a 2^{nd} order low-pass biquadratic filter with a cutoff frequency of 10 Hz and a sampling frequency of 10 MHz. These parameters are chosen to evaluate the filter's performance under extreme conditions, and moreover, understanding the limits and capabilities of this filter in this regime provides insights into the constraints and flexibilities of other filters that will be employed in the GQuEST apparatus.

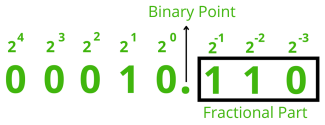

FIG. 3. Fixed-point representation example of the number 2.75. The integer part is represented by the bits to the left of the binary point, while the fractional part, boxed for emphasis, is represented by the bits to the right of the binary point. In this example, 10.11 in binary corresponds to 2.75 in decimal.

V. FIXED-POINT REPRESENTATION

To process a signal electronically, it is typical to use fixed-point representation to encode the numbers involved, as using float point could require unnecessary bits if staying within an acceptable domain of precision. Fixed-point representation consists of bits before the binary point which represent the dynamic range and of bits after the binary point which represent the precision. Additionally, there is a bit representing the sign of the encoded number.

This fixed-point representation will be used to stress-test the 2^{nd} order low-pass biquadratic filter. We will tune the bit resolution of the associated coefficients to find the threshold at which we remain within an acceptable domain.

Optimizing bit resolution is critical as it directly impacts the performance of the digital control system. Higher bit resolutions can improve the filter's precision but may also increase resource consumption, while lower resolutions save resources but risk losing important signal details. For instance, an inadequately resolved filter may introduce quantization errors, leading to less accurate signal processing and analysis.

Through this process, we aim to enhance the functionality of the control system, ensuring it can accurately and efficiently process signals from the GQuEST interferometers.

VI. DIGITAL FILTER FIXED-POINT PRECISION

A. Variance of Coefficients

For our preliminary testing of the digital filter, we chose not to use the direct form of the iterative filtering process. Instead, we focused extensively exploring the frequency response of the low-pass filter across various controlled bit resolutions. Initially, our motivation was to vary only the bit resolution of the b coefficients of our filter, as these coefficients exhibited significant variation with different critical frequencies. This variation is clearly illustrated in Figure 4.

Initially, we chose to use 1^{st} order filters due to their simplicity and accessibility. However, upon discovering that 2^{nd} order filters are as accessible and knowing that they offer greater filtering effectiveness, we transitioned from experimenting with 1^{st} order filters to 2^{nd} order filters.

As illustrated in Figures 5 and 6, varying only the b coefficients did not significantly deviate from the float behavior of the transfer functions. However, altering the resolution of

FIG. 4. Change in filter parameters (b_0, b_1, b_2, a_1, a_2) as a function of the normalized critical frequency for both 1^{st} and 2^{nd} order low-pass Butterworth filters. The x-axes and y-axes for both are scaled logarithmically. The curves for a_1 and a_2 overlay each other for both plots, while the b coefficients overlay for the 1^{st} order plot and deviate on the 2^{nd} order plot.

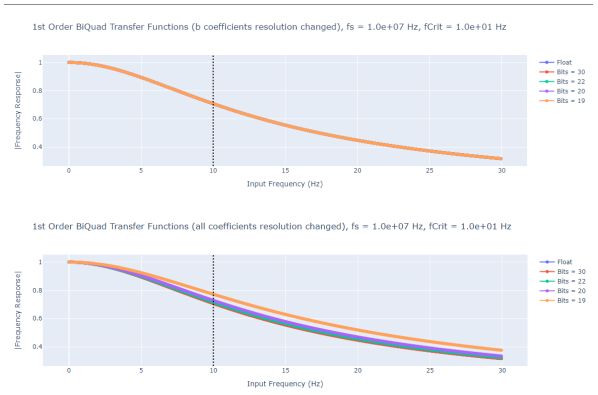

FIG. 5. Comparison of 1^{st} Order Low-Pass Transfer Functions with Varying Bit Resolution. The first plot shows changes with only the b coefficients varied, while the second plot shows changes with all coefficients varied. Both transfer functions are normalized around 0 Hz to ensure consistent filter behavior across different resolutions. Unlike the second plot, where the transfer function curves exhibit noticeable variation, the first plot shows that varying bit resolution has no effect, as all curves overlap

all associated coefficients of the filter introduced noteworthy variations that warrant further investigation. Another detail to note is the range of the bit resolutions featured in Figures 5 and 6; below a certain threshold of bit resolution, the transfer function completely attenuates the signal, outputting a zero gain for all input frequencies.

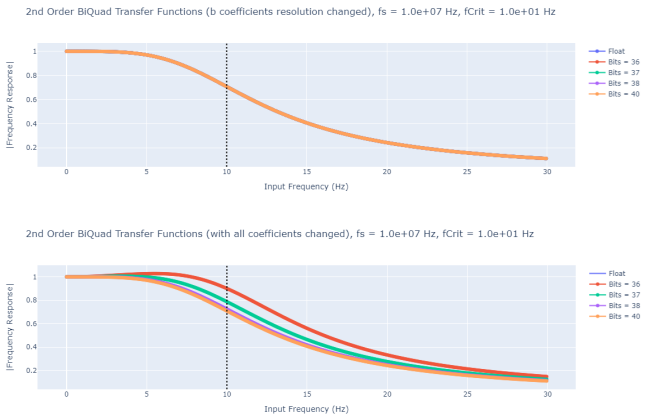

FIG. 6. Comparison of 2^{nd} Order Low-Pass Transfer Functions with Varying Bit Resolution. The first plot shows changes with only the b coefficients varied, while the second plot shows changes with all coefficients varied. Both transfer functions are normalized around 0 Hz to ensure consistent filter behavior across different resolutions. Unlike the second plot, where the transfer function curves exhibit noticeable variation, the first plot shows that varying bit resolution has no effect, as all curves overlap

B. Characterizing Deviations

Having established the domain for exploring filter behavior, we now turn our attention to characterizing the effects of reducing bit resolution on the filter performance. Specifically, we first examined the slope of the transfer function at frequencies higher than the critical frequency. For all 2^{nd} order filters, the standard roll-off is -40 dB/decade. As shown in Figure 7, adjusting the bit resolution of the filter coefficients affects the frequency at which the filter becomes effective but does not alter the slope.

Though the roll-off behavior remains unaffected, we observe slight deviations from the expected behavior. These deviations are further characterized and illustrated in Figure 8, where differences from the float-point behavior are more significant near the critical frequency.

Upon further observation of Figure 8, we notice an odd pattern in how the differences change with varying critical frequencies. Specifically, the differences exhibit a staggering behavior: they increase, then drop, and increase again, continuing this pattern as the critical frequency changes. Initially, we assumed a linear relationship between the bit resolution and critical frequency; however, this assumption did not hold true. This unexpected behavior suggests a non-linear relationship, which could have significant implications for the stability and accuracy of the filter.

Further analysis reveals that each of the curves in Figure 8 reaches a steady-state difference after growing and slightly decreasing. We leverage this characteristic and plot the averages of these steady states in Figure 9. This plot highlights the average equilibrium deviations for a spectrum of critical frequencies, providing a clearer understanding of how bit resolution impacts filter behavior across different critical frequencies for

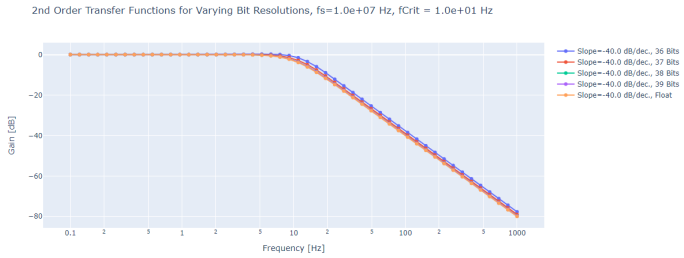

FIG. 7. Normalized Transfer Functions for Floating-Point and Lower Bit Resolution Filters. The x-axis is scaled logarithmically to highlight the standard roll-off rate of -40 dB/decade as displayed for each curve.

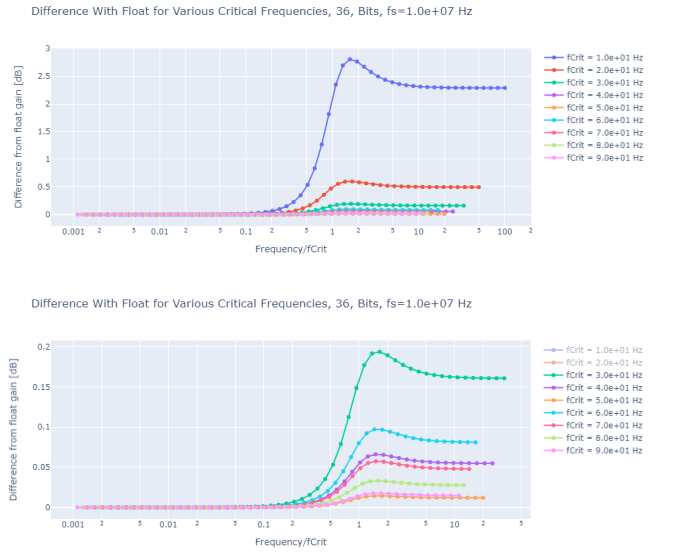

FIG. 8. Characterization of Differences Between Float Point Filter and Low-Bit Resolution Filters. The first plot displays filter behavior across critical frequencies ranging from 10 Hz to 90 Hz. The second plot isolates 30 Hz through 90 Hz critical frequencies to emphasize the varying effects at different frequencies. The x-axes of the individual curves are normalized around their respective critical frequencies, aligning the curves so that all roll-off deviations begin around frequency/fCrit = 1.

fixed bit resolutions. To ensure filtering precision within a maximum difference of 1 dB from the floating-point filter, our findings indicate that a fractional resolution of 38 bits is adequate.

C. Effects of Bit Resolution on Noise

As the GQuEST apparatus will incorporate practical filters, it is crucial to examine additional real-world factors that may influence the choice of bit resolution. One significant factor to consider is noise, which can have a substantial impact on filter performance and overall system precision.

Noise is a fundamental aspect that can impact the performance of filters, particularly in high-precision applications such as GQuEST. In the context of our study, noise introduces additional challenges that must be addressed to ensure the accuracy and reliability of the filter's output. The presence of noise can distort signal processing, affect measurement accuracy, and ultimately influence the effectiveness of the filter. Therefore, when determining an optimal bit resolution for our filter, we must also consider how it affects the filter's noise performance.

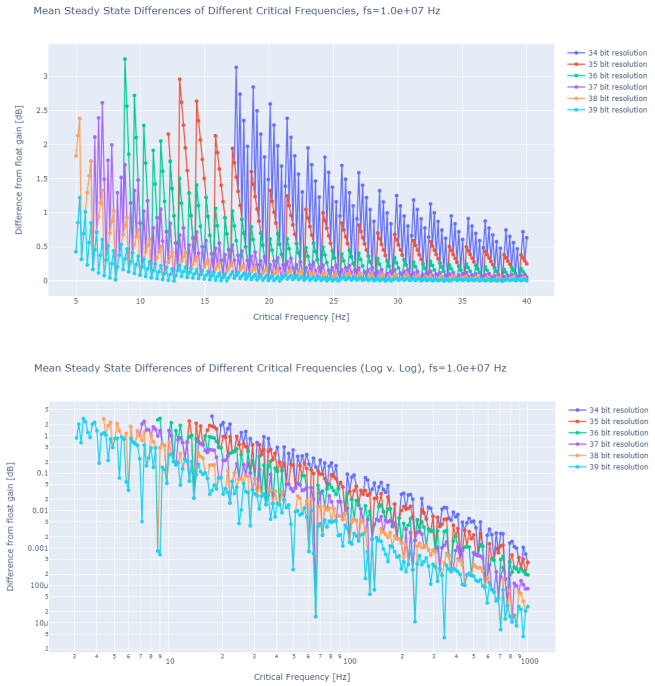

FIG. 9. Mean Steady-State Differences Between Float-Point Filter and Low-Bit Resolution Fixed-Point Filters. The top plot shows the average steady-state differences across various critical frequencies with linear scaling, while the bottom plot presents the same curves on a Log-Log scale. The linear plot displays the average steady-state differences across different critical frequencies. As shown, no steady-state behavior is evident below certain critical frequencies which is consistent with observations in Figures 5 and 6. The Log-Log plot provides a different perspective, emphasizing how the steady-state differences vary across a larger range of critical frequencies.

In the scenarios GQuEST might encounter, noise can manifest in three main forms, each with distinct implications for filter performance:

1. Alias Noise: This type of noise arises from sampling processes and can lead to distortion in signal interpretation. When the bit resolution is insufficient, alias noise can become more pronounced, affecting the accuracy of frequency domain representation and potentially causing false readings or artifacts.

2. Readout Noise: This noise is introduced during the process of reading data from sensors or measurement devices. High bit resolution can help mitigate readout

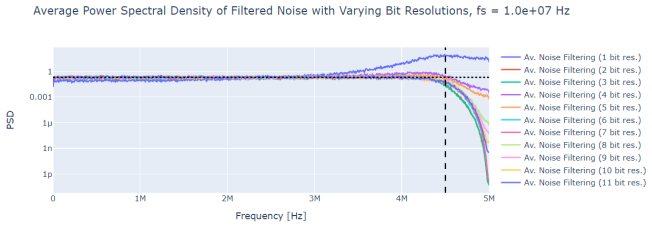

FIG. 10. Effect of Bit Resolution on Alias Noise. The plot shows the Power Spectral Density (PSD) of filtered noise across different bit resolutions, demonstrating how lower bit resolutions affect the anti-aliasing filter's performance. The PSD is computed after applying a low-pass Butterworth filter designed to attenuate frequencies above the critical frequency (90% of the Nyquist rate). The noise used in the simulation has a mean of 1 and a standard deviation of 1000.

noise by providing more precise measurements, but it also requires careful calibration to ensure that the noise does not overwhelm the signal.

3. Digitization Noise: Occurring during the analog-to-digital conversion process, digitization noise can impact the fidelity of the signal being processed. As bit resolution increases, the quantization error associated with digitization noise decreases, improving the overall accuracy of the filter. However, the trade-off between higher resolution and increased system complexity must be managed effectively.

By understanding and addressing these types of noise, we can better determine the optimal bit resolution for our filter, ensuring that it performs effectively under real-world conditions and contributes to the accuracy and reliability of the GQuEST apparatus.

From Figure 10, we observe that the effects of alias noise become significant only at very low bit resolutions, even for frequencies close to the filter's critical frequency. Thus, for the purposes of our study, alias noise can be considered negligible in the broader context of our analysis.

However, the analysis presented in Figure 11 reveals that the change in fractional bits does not significantly increase correlation with the float-point filter, indicating that the digitization noise and read noise remain prevalent regardless of the bit resolution. This suggests that while increasing the number of bits for resolution may improve certain aspects of filter performance, it does not eliminate the fundamental challenges posed by digitization and readout noise. Further strategies beyond simply increasing bit resolution are required to manage these noise effects effectively.

VII. DIGITAL FILTER FIXED-POINT DYNAMIC RANGE

Another important aspect in controlling the bit resolution of filters is exploring its effect on the dynamic range of filters. Dynamic range, which refers to the range between the smallest and largest signal levels a filter can accurately process, is

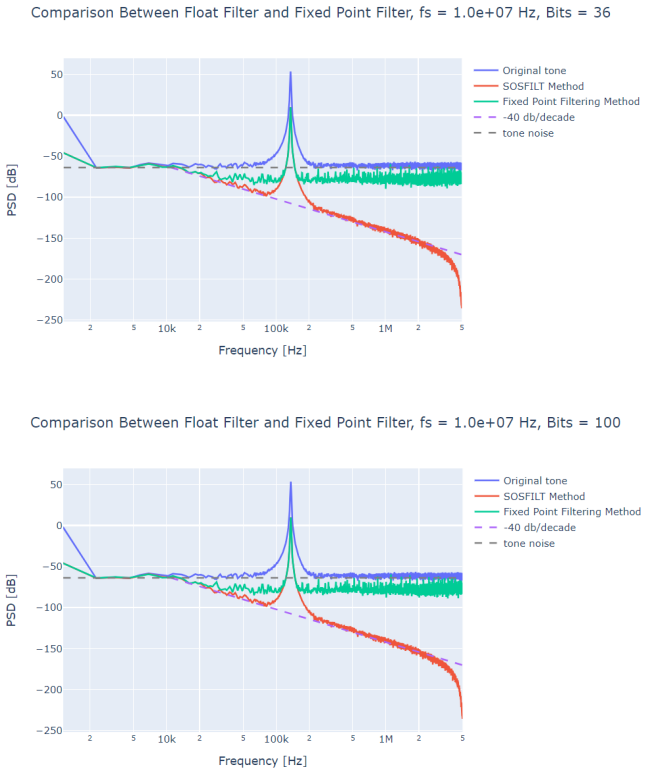

FIG. 11. Power Spectral Density Comparisons. For both, the original tone simulates typical read noise and digitization effects. The SOSFILT method is the exact performance calculated in high precision, showing roll off of amplitude by 40 dB per decade. The "Fixed Point Filtering Method" demonstrates similar behavior but limited with higher noise above ~30 kHz. The key difference between the plots is the bit resolution: one uses 36 fractional bits, while the other uses 100 fractional bits.

crucial for maintaining filter performance across varying signal strengths. The bit resolution of a filter directly impacts its dynamic range: higher bit resolutions can provide a broader dynamic range, allowing the filter to handle a wider range of signal levels without distortion. Understanding this relationship is essential for optimizing filter design, particularly in applications requiring high precision and accuracy such as GQuEST.

Specifically, bit resolution affects the filter's ability to handle signals of varying amplitudes, which can influence both overflow and underflow conditions. Overflow occurs when the filter's output exceeds the maximum representable value, while underflow happens when the output falls below the minimum value. Observations from float-point filters in Tables I and II reveal that the w_0, a_1w_1, and a_2w_2 terms from Equations 1 and 2 drastically grow in integer bit representation as the associated critical frequency of the filter decreases. This increase in bit representation with lower critical frequencies can further complicate managing overflow and underflow conditions. Conversely, other terms inside the iterative digital filtering remain constant, emphasizing that the bit resolution

challenge is particularly pronounced for the aforementioned growing terms.

The observation that the w_0, a_1w_1, and a_2w_2 components change while the b_0w_0, b_1w_1, and b_2w_2 remain stagnant seems to contradict the results from Figure 4. This discrepancy highlights the need for further investigation, as no definitive conclusion has been reached to resolve this inconsistency.

	1e6 Hz	**1e5 Hz**	**1e4 Hz**	**1e3 Hz**	**1e2 Hz**	**1e1 Hz**	**1e0 Hz**
Tone	15	15	15	15	15	15	15
y	15	15	15	15	15	15	15
w_0	17	23	30	36	43	49	56
a_1w_1	17	24	31	37	44	50	57
a_2w_2	16	23	30	36	43	49	56
b_0w_0	13	13	13	13	13	13	13
b_1w_1	14	14	14	14	14	14	14
b_2w_2	13	13	13	13	13	13	13

TABLE I. Number of integer bits required to represent terms for iterative direct form filtering with a sampling frequency of 10 MHz, 16-bit ADC, no read-noise, and a tone at 90% of maximum amplitude, across different critical frequencies.

	1e6 Hz	**1e5 Hz**	**1e4 Hz**	**1e3 Hz**	**1e2 Hz**	**1e1 Hz**	**1e0 Hz**
Tone	14	14	14	14	14	14	14
y	14	14	14	14	14	14	14
w_0	16	22	29	36	42	48	55
a_1w_1	16	23	30	36	43	49	56
a_2w_2	15	22	29	35	42	48	55
b_0w_0	12	12	12	12	12	12	12
b_1w_1	13	13	13	13	13	13	13
b_2w_2	12	12	12	12	12	12	12

TABLE II. Number of integer bits required to represent terms for iterative direct form filtering with a sampling frequency of 10 MHz, 16-bit ADC, no read-noise, and a tone at 45% of maximum amplitude, across different critical frequencies. In comparison to Table I, we see a general decreased number of integer bits, which is consistent for a lower amplitude input.

VIII. CONCLUSION

The analysis of bit resolution in the context of filter performance for the GQuEST apparatus has produced several important insights. Our research indicates that a minimum fractional bit resolution of 38 bits provides adequate precision for effective filter performance. On the other hand, further investigation is needed to fully understand how integer bit resolution affects dynamic range. This will involve directly comparing floating-point and fixed-point behaviors across various bit resolutions to identify the optimal balance between precision and resource usage.

Our findings also reveal that, despite the advantages of higher bit resolution, the practical implications of noise must be carefully considered. The observed noise behaviors—encompassing alias, readout, and digitization noise—demonstrate that increasing bit resolution alone does not entirely mitigate these effects. Specifically, while alias noise is minimal at higher bit resolutions, digitization and readout noise together persist, highlighting that further exploration and methodologies are necessary to navigate these challenges.

In summary, while a 38-bit resolution provides sufficient precision, it is crucial to continue investigating the impact of dynamic range and various noise types on filter performance. This comprehensive approach will ensure that the GQuEST apparatus achieves optimal accuracy and reliability by effectively balancing bit resolution with practical noise management strategies. Finally, understanding these technical nuances is vital for advancing our knowledge in the field of quantum gravity, as precise and reliable data acquisition and processing are foundational to exploring and validating theoretical models.

ACKNOWLEDGMENTS

I personally would like thank my supervisor, Dr. Chris Stoughton, for his patience and mentorship throughout my internship. I also extend my gratitude to Fermilab for broadening the horizons of my career through this SULI internship.

This manuscript has been authored by Fermi Research Alliance, LLC under Contract No. DE-AC02-07CH11359 with the U.S. Department of Energy, Office of Science, Office of High Energy Physics.

This work was supported in part by the U.S. Department of Energy, Office of Science, Office of Workforce Development for Teachers and Scientists (WDTS) under the Science Undergraduate Laboratory Internships Program (SULI).

[1] K. M. Zurek, "On vacuum fluctuations in quantum gravity and interferometer arm fluctuations," Physics Letters B **826**, 136910 (2022).
[2] E. P. Verlinde and K. M. Zurek, "Observational signatures of quantum gravity in interferometers," Physics Letters B **822**, 136663 (2021).
[3] S. M. Vermeulen, T. Cullen, D. Grass, I. A. O. MacMillan, A. J. Ramirez, J. Wack, B. Korzh, V. S. H. Lee, K. M. Zurek, C. Stoughton, and L. McCuller, "Photon counting interferometry to detect geontropic space-time fluctuations with gquest," (2024), arXiv:2404.07524 [gr-qc].